PCIM Europe 2018; International Exhibition and Conference for Power Electronics, Intelligent Motion, Renewable Energy and Energy Management; Proceedings of

Protection Schemes in Low-Voltage DC Shipboard Power Systems

S. Kim, D. Dujic, and S. Kim

POWER ELECTRONICS LABORATORY
ÉCOLE POLYTECHNIQUE FÉDÉRALE DE LAUSANNE

Protection Schemes in Low-Voltage DC Shipboard Power Systems

Seongil Kim*, Dražen Dujić*, Soo-Nam Kim**
*Power Electronics Laboratory, École Polytechnique Fédérale de Lausanne (EPFL), Switzerland
**Power Control Research Department, Hyundai Electric, Repulic of Korea
seongil.kim@epfl.ch, drazen.dujic@epfl.ch, kimsoonam@hyundai-electric.com

Abstract

Shipbuilding industry has increased interest into DC shipboard power systems (SPS) for their benefits, such as improved fuel efficiency and installation footprint. These new power systems come with technical challenges in system protection owing to lack of natural zero crossing in case of DC fault currents and low thermal capability of semiconductors. This paper presents feasible protection schemes against DC short circuit faults for three different types of, commercially available, low-voltage DC (LVDC) rectifier systems: a six-pulse diode rectifier, a six-pulse thyristor rectifier and a two-level active rectifier. In addition, a novel protection method, which provides a simply way for limiting fault currents, is proposed and discussed for the active rectifier

1. Introduction

A DC network has been considered as a promising solution for the next-generation SPSs with its main benefits in marine domain, such as high fuel efficiency with variable-speed engines, better integration of energy storage systems and footprint savings in electrical equipment by removing bulky transformers [1]–[3]. Recently, various LVDC solutions have been introduced to dynamic positioning vessels (i.e. platform supply vessels and shuttle tankers) with power levels up to $20\,\mathrm{MW}$ and a DC voltage level of $1\,\mathrm{kV}$ [4], [5]. A simplified schematic of the LVDC SPS is depicted in Fig. 1. It consists of generators, rectifiers, hotel loads, large motors, thrusters, energy storage systems and a bus tie breaker.

One of major challenges in this new concept of power systems is the power system protection which is to keep the power system stable and minimize the impact from system faults by selectively isolating a faulty part. This is due to no natural current zero-crossing of a fault on the DC network and very low thermal capability of semiconductors in power converters. To overcome these technological barriers, a lot of researches have been conducted. However, there is still a lack of comprehensive studies on DC protection schemes concerning thermal capability of semiconductors and short circuit energy limited by protection measures.

This paper presents two protection schemes for the diode and the thyristor rectifier-based LVDC SPSs, shown in Fig. 2 (a) and (b), respectively. In addition, a novel protection scheme for the active recfier-based SPS shown in Fig. 2 (c) is proposed. The proposed method uses an artificial three-phase short circuit on the AC-side to interrupt the fault current passing through the power converter. Protection schemes taken into account in this paper are evaluated by fault and thermal capability analysis. Note that this paper does not discuss protection coordination (or time coordination) and backup protection for whole LVDC SPSs under loading conditions, but aim to present feasible DC short circuit protection schemes depending on the rectifier type.

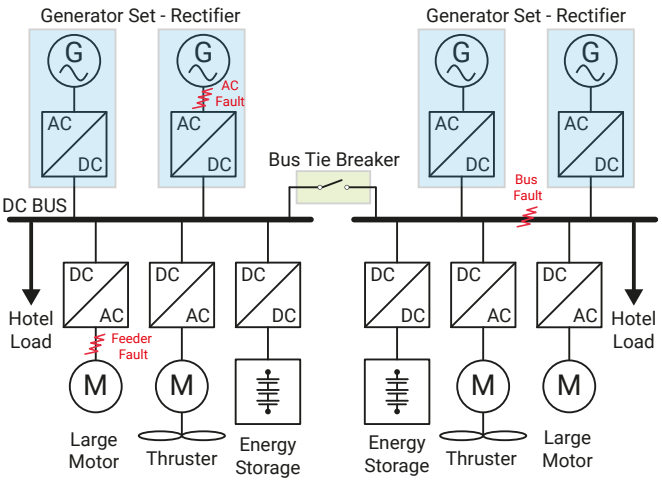

Fig. 1: Simplified schematic of LVDC SPS [6].

ISBN 978-3-8007-4646-0

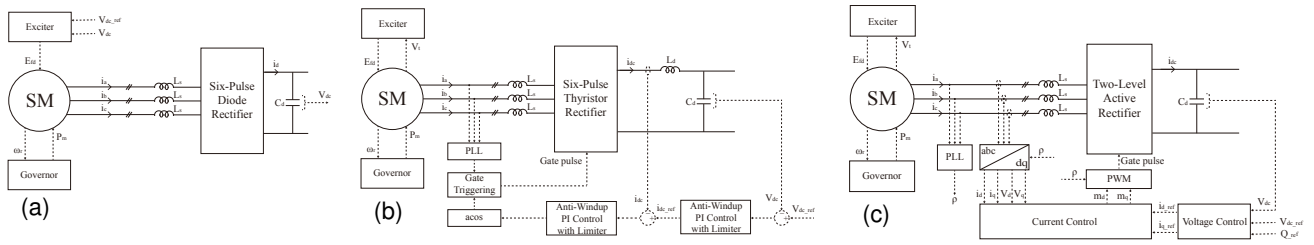

Fig. 2: Different DC shipboard power generation systems combined generator sets and source side converters [7]: (a) six-pulse diode rectifier, (b) six-pulse thyristor rectifier and (c) two-level active rectifier.

2. Protection Schemes

The faults in the LVDC SPSs are divided into three types shown in Fig. 1: AC faults, DC bus faults and feeder faults. The AC faults, such as synchronous generator and AC cable failures between a generator and a rectifier, have to be cleared by conventional AC protection devices (generator protection units or/and protective relays with AC circuit breakers). The feeder faults are handled by high-speed semiconductor fuses to protect inverters and electrical loads. In DC protection, more attention should be paid to the DC bus faults because the management of the bus faults are much more difficult than the other faults due to their higher fault currents and very low thermal (or overcurrent) withstand ratings of power converters.

For the DC bus fault, the bus tie breaker in Fig. 1 autonomously separates each bus within a few tens of microseconds [5], and then the voltage in the healthy bus is ramped up again to be independently operated. In the faulty part, the fault is isolated by means of different protection schemes depending on the converter topologies and overall energy management strategy on the ship. Several protection strategies have been already proposed in the literature [4], [5], and they generally need to be analysed in relation to the type of rectifier that is used in the system.

2.1. Diode rectifier-based SPS

In [5], the protection scheme for the diode rectifier-based LVDC SPS in Fig. 2 (a) is described. The protection scheme uses a synchronous generator specially designed with high subtransient direct-axis reactance and the excitation removal function.

Considering a relatively high value of the direct-axis subtransient time constant (typically, around $35\,\mathrm{ms}$ [8]) compared with a fault clearance time of the DC faults, the DC fault current i_{DC} provided by the synchronous generator is mainly governed by the subtransient reactance value $X_d^{''}$ as [9]:

$$i_{DC} = \frac{3\sqrt{2}}{\pi} \frac{V_{LN}}{\sqrt{R_s^2 + \left(X_d^{''} + X_f\right)^2}} \tag{1}$$

where, V_{LN} is the RMS value of line-to-ground AC voltage, R_s is the source resistance, and X_f is the AC-side reactance. In other words, the fault energy contributed by the generator is significantly decreased with the increased subtransient reactance.

A generator protection unit, on the other hand, removes the excitation for eliminating the fault current contribution from the synchronous generator, when the overload condition is detected. In case of a brushless excitation system, the flux linkage in the field winding of the synchronous generator starts to naturally discharge after the excitation removal and it results in slow decay in the fault contribution. Meanwhile, a direct (or static) excitation system based on thyristor rectifier has fast response characteristics as well as immediate de-excitation function. The excitation removal fault-limiting method, therefore, is more effective for the synchronous generator with the direct excitation, yet it is still relatively slow method and not sufficient on its own.

2.2. Thyristor rectifier-based SPS

The thyristor rectifier shown in Fig. 2 (b) can adjust the DC link voltage by manipulation of the firing angle. Furthermore, the firing angle control is also applicable to the DC fault management. The thyristor rectifier can reverse DC voltage polarity in a very short time by forcing the firing angle into $110°$-$120°$ [9], called fold-back protection control.

The protection scheme proposed in [4] is based on the fold-back control of the thyristor rectifier to extinguish the DC fault current. With this control, a "breaker-less" power system can be achieved for the thyristor rectifier-based LVDC SPS.

2.3. Active rectifier-based SPS

There are two feasible protection methods for the active rectifier based-SPS shown in Fig. 2 (c): i) a fault-blocking converter with a DC isolator and ii) a conventional converter with an increased AC coupling reactor. The modular multi-level converter based on full-bridge cells can block the DC fault current to zero and the high-speed DC isolator provides galvanic isolation (or electrical isolation). The fault-blocking converter, however, has higher costs and conduction losses. Larger AC coupling reactor is necessary for the conventional converter with the slow speed AC breaker because the reactor can reduce the fault current level. But, the reactor decreases the converter utilization ratio [9], which is defined as the ratio of the output power divided by the input power of the power converter. Thus, higher power rating of the converter is necessary for the increased AC reactor.

In order to overcome the aforementioned drawbacks of the protection methods, the artificial short circuit protection method depicted in Fig. 3 is proposed. When the DC fault is detected, the internal protection of the active rectifier blocks the operation of the IGBT switches by removing PWM pulses and then the rectifier acts as a diode rectifier. The anti-parallel diodes in the rectifier experience the fault current shown in Fig. 3. The proposed method enables the interruption of the fault current passing through the diodes by developing the three-phase short circuit between the AC reactor and the rectifier. The artificial short circuit provides other current path (orange-colored dot lines in Fig. 3) with almost zero impedance within $4\,\mathrm{ms}$ [10], if a high-speed mechanical earthing switch is used for the short circuit. By coordinating the semiconductor thermal rating with the fault energy during this period, the proposed method provides an effective way for the DC protection. Finally, the AC breaker separates the generator from the artificial short circuit.

This method needs to install the AC breaker and the artificial short circuit device for every single generator. Thus, there may be a cost trade-off issue between the proposed method and the mechanical DC breaker, which is available up to $3.6\,\mathrm{kV}$ and developed for the railway application [11]. But, the proposed method can simply interrupt the fault current faster than the DC breaker and it gives a significant benefit to handle the fault energy.

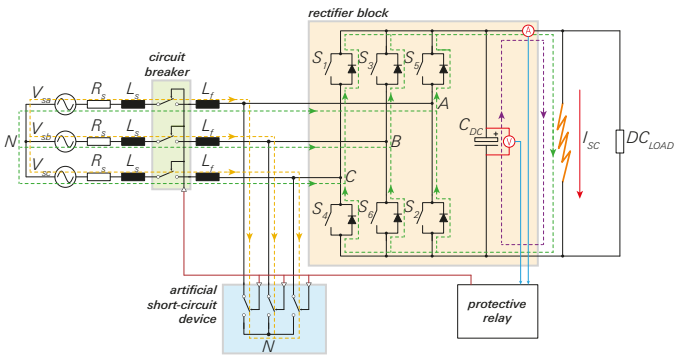

Fig. 3: Schematic diagram of artificial short circuit protection method.

3. Thermal Withstand Capability

Power converters based on semiconductors have much lower fault current withstand capability than that of other power equipment such as generators, transformers and cables, as shown in Fig. 4. It means that the power converter is critical bottleneck compared to other equipment with much larger thermal capability that allows for overloading. There-

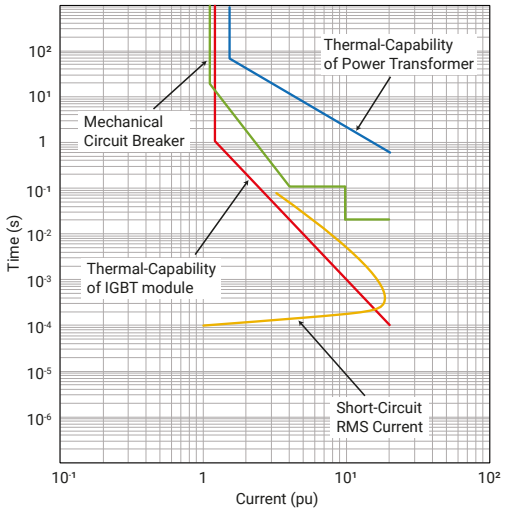

Fig. 4: Time-current characteristics for IGBT, transformer and circuit breaker [6].

Table 1: High-power semiconductor data chosen for the considered rectifiers

Device	Rated Voltage V_{RSM}, V_{DRM} or V_{CES} (V)	Rated Current $I_{F(AV)M}$, I_C or $I_{T(AV)M}$ (A)	Peak Surge Current I_{FSM} or I_{TSM} (kA)	Limiting Load Integral I^2t (A^2s)
Diode - 5SDD 51L2800 [12]	2800	5380	65.0	$21.13 \cdot 10^6$
Thyristor - 5STP 45Q2800 [13]	2800	5490	77.0	$29.64 \cdot 10^6$
IGBT - 5SNA 3600E170300* [14]	1700	7200	36.0	$6.48 \cdot 10^6$

* Note: Two IGBTs in parallel

fore, thermal capabilities of relevant semiconductor devices are analysed in relation to fault energies and implications on the overall system design.

For the rectifiers from Fig. 2, the semiconductor devices from Table 1 are chosen to handle the rated DC current ($4\,\mathrm{kA}$ given in Table 2) and the rated line voltages (the AC voltages). The line voltages are dependent on the rectifier topologies to obtain a same DC voltage. Hence, different ratings of the line voltage are selected to achieve the rated DC voltage ($1000\,\mathrm{V}$ given in Table 2) as: $740\,\mathrm{V}$ for the diode rectifier, $850\,\mathrm{V}$ for the thyristor rectifier, and $480\,\mathrm{V}$ for the active rectifier.

Among the three devices in Table 1, the ratings of the peak surge current and the limiting load integral, which provide information on the fault current withstand capability of semiconductors, are highest for the thyristor, while they are lowest for the IGBT with anti-parallel diode. One should note that DC faults in the active rectifier have to be cleared much faster than the diode and the thyristor rectifiers.

4. Fault simulation and comparison

To evaluate the protection schemes presented in Section 2, the three generator-rectifier systems in Fig. 2 are modelled by EMTP-RV [18] with the parameters as in Table 2. The modelling of the control systems for the rectifiers is performed in connection with the set of the exciter and the governor, as illustrated in Fig. 2.

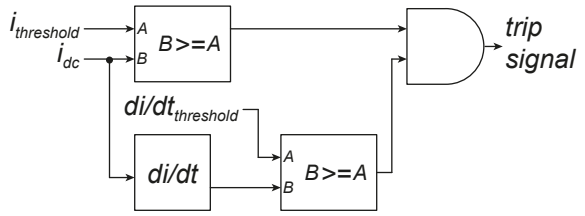

Fig. 5: Fault detection based on current amplitude and its derivative.

In DC networks, fast fault detection is necessary to ensure the safety of the semiconductors. For this reason, a fault detection method based on current amplitude and its derivative, which can determine the fault occurrence in a very short period of time, is implemented as shown in Fig. 5. The thresholds of the amplitude and the derivative used in this paper are $1.5\,\mathrm{pu}$ and $2.0 \cdot 10^5\ \mathrm{pu/s}$, respectively.

Table 2: Parameters used for the study

System parameter			
Rated generator power	$5\,\mathrm{MVA}$		
Rated rectifier power	$4\,\mathrm{MW}$		
Rated DC voltage	$1\,\mathrm{kV}$		
Rated AC frequency	$60\,\mathrm{Hz}$		
AC-side inductor	$0.1\,\mathrm{pu}$ (at $5\,\mathrm{MVA}$ base)		
DC link capacitor	$0.0553\,\mathrm{mF}$ (only for thyristor rectifier)		
Synchronous machine taken from [15]			
X_d	$1.56\,\mathrm{pu}$	X_l	$0.052\,\mathrm{pu}$
$X_d^{'}$	$0.296\,\mathrm{pu}$	X_q	$1.06\,\mathrm{pu}$
$X_d^{''}$	$0.177\,\mathrm{pu}$	$X_q{}'$	$0.177\,\mathrm{pu}$
$T_d^{'}$	$3.7\,\mathrm{s}$	$T_q^{'}$	$0.05\,\mathrm{s}$
$T_d^{''}$	$0.05\,\mathrm{s}$	R_s	$0.0036\,\mathrm{pu}$
Brushless exciter (IEEE AC5A) taken from [16]			
K_A	$400\,\mathrm{pu}$	T_A	$0.02\,\mathrm{s}$
V_{Rmax}	$7.3\,\mathrm{pu}$	K_E	$1.0\,\mathrm{pu}$
V_{Rmin}	$-7.3\,\mathrm{pu}$	T_E	$0.1\,\mathrm{s}$
K_F	$0.03\,\mathrm{pu}$	$S_E[E_{FD1}]$	$0.86\,\mathrm{pu}$
T_{F1}	$1.0\,\mathrm{s}$	E_{FD1}	$5.6\,\mathrm{pu}$
T_{F2}	$0\,\mathrm{s}$	$S_E[E_{FD2}]$	$0.5\,\mathrm{pu}$
T_{F3}	$0\,\mathrm{s}$	E_{FD2}	$4.2\,\mathrm{pu}$
Diesel-engine governor taken from [17]			
K_p	$40\,\mathrm{pu}$	T_D	$0.024\,\mathrm{s}$
T_{1c}	$0.01\,\mathrm{s}$	T_{1a}	$0.25\,\mathrm{s}$
T_{2c}	$0.02\,\mathrm{s}$	T_{2a}	$0.009\,\mathrm{s}$
T_{3c}	$0.2\,\mathrm{s}$	T_{3a}	$0.0384\,\mathrm{s}$
T_{min}	$0\,\mathrm{pu}$	T_{max}	$1.1\,\mathrm{pu}$

4.1. Simulation cases

Fault simulation cases for each LVDC solution are presented in Table 3. The protection schemes for the diode rectifier solution are studied as Cases 1.1, 1.2 and 1.3. In Case 1.1, the excitation removal with normal subtransient reactance ($X_d'' = 0.177\,\mathrm{pu}$) is analysed to check the impact of the high subtransient reactance. For Case 1.2, 1.5 times of X_d'' is assumed for the implementation of the method in [5]. Considering relatively high thermal withstand capability of the diode, an AC circuit breaker operation can be a feasible solution. The AC breaker solution with the trip time of $50\,\mathrm{ms}$, therefore, is investigated in Case 1.3.

The fold-back protection control for the thyristor rectifier is studied in Case 2.1. The firing angle of $120°$ is forced with time delay of $1\,\mathrm{ms}$ after the fault detection. The AC breaker solution is also examined for the thyristor rectifier in Case 2.2.

For the active rectifier, the AC breaker solution is analysed in Case 3.1. The proposed artificial three-phase short circuit on the AC-side is investigated in Case 3.2, and the operation time of $10\,\mathrm{ms}$ is considered for this method.

In SPSs, the continuous power supply is an important for the safety. To prevent the power interruption from a single line to ground fault, the unearthed system is mainly used in ships and offshore platforms. A pole-to-pole fault in the DC side, therefore, is considered with fault resistance of $0.015\,\Omega$.

Table 3: Simulation cases for the considered rectifiers

LVDC Solution	Case	Description
Diode rectifier	1.1	Excitation removal with normal X_d''
	1.2	Excitation removal with high X_d''
	1.3	AC breaker trip
Thyristor rectifier	2.1	Fold-back protection control (α =120°)
	2.2	AC breaker trip
Active rectifier	3.1	AC breaker trip
	3.2	Artificial short circuit (Proposed method)

4.2. Simulation results

The simulation results are presented in Fig. 6. The short circuit current in Fig. 6 (a), (c) and (e) is the fault current on the side of the DC fault. In Fig. 6 (b), (d) and (f), the maximum through-fault energy among the six semiconductors is compared with the thermal withstand capability of the semiconductors in Table 1. These results are applicable to selected semiconductor devices, and thus should not be considered to be of general nature. Every design should be analysed on a case by case basis.

The impact of the high subtransient reactance is presented in Fig. 6 (a) and (b). The high subtransient reactance can significantly reduce the initial fault current as well as the short circuit energy compared with the normal subtransient reactance case. With the excitation system used in this paper, it takes a few tens of seconds to completely extinguish the fault current with the excitation removal. Several diodes in parallel, thus, are needed to sustain the fault current for such a long time and the high short circuit energy to avoid any device damages. Otherwise, a fast flux discharging method should be considered to reduce the fault current contribution of the synchronous machine (i.e. the direct excitation system). On the other hand, the AC breaker solution in Case 1.3 can interrupt the fault current with an enough safety margin.

The fold-back protection control for the thyristor rectifier (Case 2.1) can promptly interrupt the fault current, as shown in Fig. 6 (c). Fig. 6 (d) shows that the short circuit energy limited by the fold-back protection control ($0.58 \cdot 10^6 A^2 s$) is much less than the rating of the thyristor thermal capability ($29.64 \cdot 10^6 A^2 s$ in Table 1). The AC breaker solution in Case 2.2 is also effective to deal with the DC fault in the thyristor rectifier. The staircase-shaped waveform (blue line in Fig. 6 (d)) is from an six-pulse interval of the thyristor rectifier.

In Case 3.1, the simulation results in Fig. 6 (e) and (f) show that at least three IGBT modules in parallel are required for the active rectifier due to its low thermal capability and the slow operation of the AC breaker. The artificial three-phase short circuit is generated at $10\,\mathrm{ms}$ after the fault detection for Case 3.2, and it limits the fault contribution from the source to the fault, as illustrated in Fig. 6 (e). With

ISBN 978-3-8007-4646-0

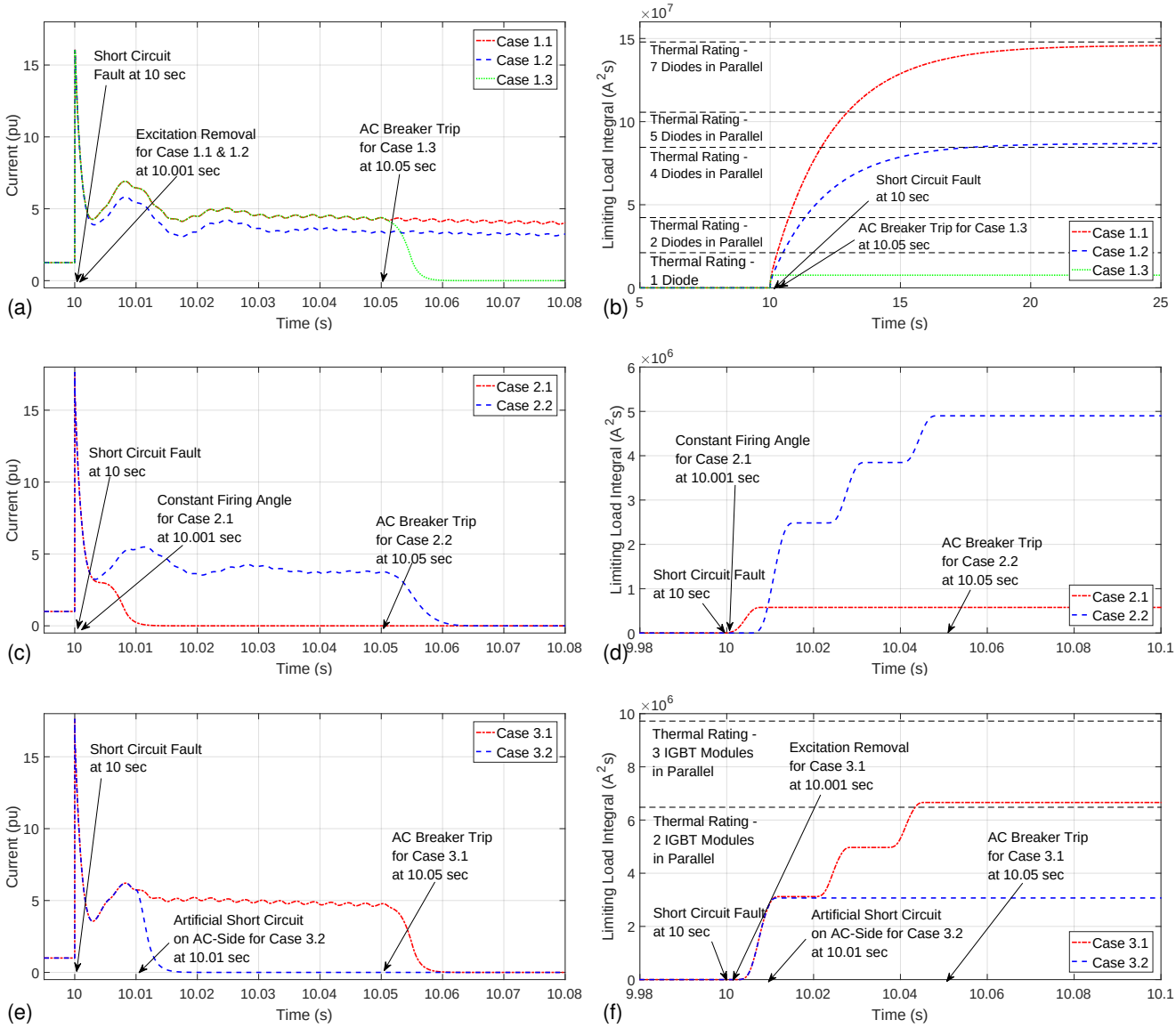

Fig. 6: Short circuit analysis with thermal capability comparison: (a) short circuit current for the diode rectifier, (b) short circuit energy for the diode rectifier, (c) short circuit current for the thyristor rectifier, (d) short circuit energy for the thyristor rectifier, (e) short circuit current for the active rectifier, and (f) short circuit energy for the active rectifier.

this fault limitation, the proposed method can control the fault energy below a half of the IGBT module rating (Fig. 6 (f)) that the anti-parallel diode is a critical part after the IGBT blocking.

5. Conclusion

This paper presented, proposed and compared the protection schemes for the three different LVDC SPSs with the fault and thermal capability analysis. The overview of the protection schemes for the diode and the thyristor rectifiers was briefly provided, and the novel protection scheme for the active rectifier was introduced. With the system modelling, the DC short circuit analyses were carried out for the several protection schemes, and each protection scheme was evaluated by comparing the short circuit energy limited by the protection operation with the thermal withstand capability of the semiconductors.

To employ the excitation removal method, the synchronous machine has to be specially designed to manage the fault contribution within the semiconductor thermal rating. In the absence of the fast flux discharging method, it takes a long time (several tens of seconds) to extinguish the fault cur-

rent in the analysis. Meanwhile, the fault isolation with the AC breaker can be a feasible solution for the diode rectifier-based LVDC SPS. The thyristor rectifier has a competitive advantage in the system protection due to its fault blocking function and high thermal withstand capability. Both protection schemes (the fold-back control and the AC breaker solution) studied in this paper were validated for the thyristor rectifier-based LVDC SPS and they can be adapted for the primary protection and the backup protection. For the active rectifier, the AC breaker solution alone is not appropriate because of the very low thermal withstand capability of the IGBT module. While the simulation result for the proposed protection method showed that the method provides a great performance for limiting the fault energy and can be a promising protection scheme for the active rectifier-based LVDC SPS.

Acknowledgment

This work was supported by Hyundai Electric Co., LTD., Republic of Korea.

References

[1] Z. Jin, G. Sulligoi, R. Cuzner, L. Meng, J. C. Vasquez, and J. M. Guerrero, "Next-Generation Shipboard DC Power System: Introduction Smart Grid and DC Microgrid Technologies into Maritime Electrical Networks," *IEEE Electrification Magazine*, vol. 4, no. 2, pp. 45–57, Jun. 2016.

[2] R. Prenc, A. Cuculić, and I. Baumgartner, "Advantages of using a DC power system on board ship," *Pomorski zbornik*, vol. 52, no. 1, pp. 83–97, 2016.

[3] B. Zahedi, L. E. Norum, and K. B. Ludvigsen, "Optimized efficiency of all-electric ships by dc hybrid power systems," *Journal of Power Sources*, vol. 255, no. Supplement C, pp. 341–354, 2014.

[4] J. F. Hansen, J. O. Lindtjørn, and K. Vanska, "Onboard DC grid for enhanced DP operation in ships," in *Dynamic Positioning Conference, Houston*, 2011.

[5] S. O. Settemsdal, E. Haugan, K. Aagesen, and B. Zahedi, "New Enhanced Safety Power Plant Solution for DP Vessels Operated in Closed Ring Configuration," in *Dynamic Positioning Conference, Houston*, 2014.

[6] S. Kim, D. Dujic, Y. Park, and S.-N. Kim, "Review of Protection Coordination Technologies in DC Distribution Systems," in *24th International Conference on Electrical Engineering (ICEE 2018)*, 2018.

[7] U. Javaid, F. D. Freijedo, D. Dujic, and W. van der Merwe, "Dynamic Assessment of Source-Load Interactions in Marine MVDC Distribution," *IEEE Transactions on Industrial Electronics*, vol. 64, no. 6, pp. 4372–4381, 2017.

[8] H. Saadat, *Power System Analysis*, ser. McGraw-Hill series in electrical and computer engineering. McGraw-Hill, 2002.

[9] D. Jovcic and K. Ahmed, "Fault Management and HVDC System Protection," in *High-Voltage Direct-Current Transmission*. John Wiley & Sons, Ltd, 2015, pp. 98–106.

[10] *Ultra-Fast Earthing Switch UFES*, ABB, Sep. 2016. [Online].

[11] *High–Speed DC Circuit Breaker for 3 kV$_{DC}$ rolling stock*, Secheron, 2015. [Online].

[12] *Rectifier Diode-5SDD 60Q2800*, ABB, Apr. 2013. [Online].

[13] *Phase Control Thyristor-5STP 45Q2800*, ABB, Mar. 2014. [Online].

[14] *HiPak IGBT Module-5SNA 3600E170300*, ABB, Feb. 2014. [Online].

[15] A. Cuculić, J. Ćelić, and R. Prenc, "Marine Diesel-generator Model for Voltage and Frequency Variation Analysis During Fault Scenarios," *Pomorski zbornik*, vol. 51, no. 1, pp. 11–24, 2016.

[16] "IEEE Recommended Practice for Excitation System Models for Power System Stability Studies," *IEEE Std 421.5-2016 (Revision of IEEE Std 421.5-2005)*, pp. 1–207, 2016.

[17] J. Alsaihati, "Simulation and Economic Analysis of a Hybrid Wind Diesel System for Remote Area Power Supply," Master's thesis, National Sun Yat-Sen University, 2010.

[18] J. Mahseredjian, V. Dinavahi, and J. A. Martinez, "Simulation Tools for Electromagnetic Transients in Power Systems: Overview and Challenges," *IEEE Transactions on Power Delivery*, vol. 24, no. 3, pp. 1657–1669, 2009.

